Contemporary Physics, 2002, volume 43, number 5, pages 351–364

Taylor & Francis
Taylor & Francis Group

Self-assembled semiconductor quantum dots

Richard J. Warburton

Quantum dots are nanometre-sized clusters of semiconductor material which confine electrons in all three directions. The physics of quantum dots are dominated by quantization: there are discrete energy levels, as in real atoms. Quantum dots can now be self-assembled directly in the growth of inorganic semiconductors, and this discovery has fuelled an explosion in the interest in this field. A review of some of this work is presented, concentrating on the optical properties of quantum dots, and possible applications for photonic devices.

1. Introduction

Quantum dots combine two contemporary themes. First, they are nanometre-sized in all three directions. Secondly, they can be produced by self-assembly, meaning that under certain conditions the dots form spontaneously. The discovery of the self-assembly of quantum dots has opened up a range of new possibilities in semiconductor physics and may well lead to a new range of photonics devices. The important concept is quantization: for sufficiently small quantum dots, there is a series of discrete electronic energy levels. Nonetheless, a quantum dot is typically buried in a semiconductor environment, and this allows the atom-like properties of quantum dots to be combined with semiconductor heterostructures, stacks of different semiconductors designed for a particular application. On the one hand, it is possible to design sophisticated experiments on these artificial atoms in order to probe the detailed electronic structure; on the other hand, the dots can be introduced into tried-and-tested semiconductor heterostructures for photonic devices.

Semiconductors are very versatile materials for electronic applications. Until the 1960s, semiconductor devices consisted essentially of bulk materials, functionalized by introducing a doping profile. However, it was recognized that there would be considerable advantages in making semiconductor heterostructures consisting of layers of different semiconductors where each layer is defect free and possibly just a few tens of nanometres thick. This work was pioneered by Zhores I. Alferov and Herbert Kroemer who were awarded the Nobel prize in 2000 'for developing semiconductor heterostructures used in high-speed and opto-electronics' (see for example, the instructive web site [1]). The fundamental idea is to exploit electron quantization; when an electron is confined between two potential barriers, the continuous energy spectrum breaks up into discrete levels. The crucial concept is the density of states (see, for example, [2]), the number of available energy levels in a particular small energy range, and the density of states is radically changed in semiconductor heterostructures compared with bulk materials. In a quantum well for instance, consisting of a thin layer of one material of low bandgap sandwiched between a material of higher band gap, the electrons confined to the thin layer are free to move in only two dimensions, their motion being quantized in the third direction, and this has a dramatic effect on the density of states.

The physics of two-dimensional electron gases in semiconductors has been studied extensively ever since the first samples were available [3, 4], and this has led to both fundamental new discoveries, for instance the quantum Hall effect [5] and the fractional quantum Hall effect [6], and much improved devices, for instance laser diodes and low-noise high-speed transistors [7]. The workhorse in the research community is the GaAs material system. AlAs has almost the same lattice constant as GaAs but a larger band gap, allowing heterostructures to be built up. In fact, the technique of epitaxy, the growth of one atomic layer at a time, has been perfected in the GaAs system, and materials of unparalleled quality can be produced.

The growth technology for semiconductor heterostructures can be extended to include other materials where the constraint of lattice mismatch is lifted. For instance, thin

Author's address: Department of Physics, Heriot–Watt University, Edinburgh EH14 4AS, UK; E-mail: R.J.Warburton@hw.ac.uk

Contemporary Physics ISSN 0010-7514 print/ISSN 1366-5812 online
http://www.tandf.co.uk/journals
DOI: 10.1080/0010751021012384 5

$In_xGa_{1-x}As$ layers can be grown on GaAs with excellent crystal quality even though the $In_xGa_{1-x}As$ lattice constant is considerably larger than that of GaAs. The $In_xGa_{1-x}As$ layer is obviously strained, and the strain energy is sufficient to nucleate dislocations once a certain thickness has been reached, typically 100–200 nm for a 1% lattice mismatch. The self-assembly of quantum dots was discovered by growing highly strained layers, for instance InAs on GaAs where the lattice mismatch is some 7%. After the growth of only a few monolayers, the InAs layer becomes highly dislocated with very poor optical properties. At smaller coverages however, quantum dots were discovered, nanometre-sized islands of indium-rich material. Remarkably, the quantum dots are very uniform, with only small fluctuations in diameter and height from one to the next. This discovery has ignited an explosion in research into the physics of quantum dots, and there are now a large number of groups working in this field. The aims are to understand the fundamental physics of these new systems and to exploit their new properties for photonics devices.

This paper makes an attempt to review the fast-moving field of self-assembled semiconductor quantum dots. The aim has been to present a coherent story rather than to produce a definitive review. The bibliography is therefore very limited, and in no way does justice to the large number of groups which have made valuable contributions to this field. The emphasis is on the interaction of quantum dots with light, as this is where the quantization is most immediately apparent, and where it might be most easily exploited for devices.

2. Quantization in quantum dots

An individual atom has a set of discrete energy levels. Conversely, a semiconductor has energy bands through the overlapping and hybridization of the individual atomic levels (see, for example, [2]). A quantum dot contains typically hundreds of atoms, and therefore the starting point for a discussion of the quantum dot's electronic properties is the band structure of the host material rather than the discrete levels of individual atoms. In the so-called effective mass approximation, this amounts to giving both electrons and holes a quadratic dispersion on wave vector k, just as for free electrons, but with an effective mass, typically about 0.1 for electrons and 0.3 for holes [3]. However, an electron in a quantum dot does not behave like an electron in bulk material because the quantum dot represents a confining potential, and this gives rise to quantized states with wavefunctions localized at the quantum dot. Significantly, self-assembled quantum dots are small enough that quantization effects are important: the energy separation between the electronic levels is larger than the other important energy scales in the system, and in particular the thermal energy.

A simplified picture therefore is that of a particle with a particular effective mass moving in a three-dimensional confining potential. At present, the exact form of the confining potential is unknown, and in any case it varies from system to system, and even from quantum dot to quantum dot within the same sample, but hints as to its form can be gleaned by interpreting optical spectroscopy. For lens-shaped InAs dots on GaAs, the confining potential is soft and roughly parabolic in the plane, and relatively hard in the growth direction. To a first approximation, the quantum dot represents a two-dimensional harmonic oscillator. This model works well for lens-shaped InAs dots, but less well for others, in particular for dots with facets.

In addition to the level separation, an important parameter is the energy barrier separating a confined state from the continuum of energy levels at higher energy. The continuum arises from the semiconductor material surrounding the quantum dots. In fact, self-assembled quantum dots sit in a so-called wetting layer, essentially a very thin epitaxial-layer (epilayer) connecting all the dots. This behaves like a disordered quantum well; therefore it has a broad density of states and represents the continuum for self-assembled systems. The barrier height in addition to the dot size determines the number of confined levels. Also, the thermal excitation of electrons or holes out of a quantum dot depends on the ratio of the barrier height to the thermal energy. This barrier height can be up to several hundred millielectronvolts (meV). This means that, at low temperatures, an electron has a very small probability of being thermally excited out of one particular quantum dot and, if a certain number of electrons are excited randomly into an ensemble of quantum dots, they will never come into thermal equilibrium in the lifetime of a typical measurement [8]. On the other hand, thermal excitation is much faster at room temperature, where the barrier heights are typically not high enough to prevent the system from reaching thermal equilibrium.

3. Self-assembly of quantum dots

When growing one material on top of another, three principal growth mechanisms have been identified: Frank–van der Merwe, Volmer–Weber and Stranski–Krastanov modes. In the Frank–van der Merwe mode, material is deposited layer by layer, as in the growth of the lattice-matched pair GaAs and AlAs. In the Volmer–Weber mode, island formation occurs: the material does not wet the surface because it is energetically unfavourable. Another possibility arises if there is a lattice mismatch. In this case, the epilayer is strained, and the strain energy obviously increases with increasing epilayer thickness. In the Stranski–Krastanow mode, the initial growth is layer by layer, as in the Frank–van der Merwe mode, but beyond a certain

thickness, the so-called critical thickness, islands form, as shown schematically in figure 1. The island formation limits the strain energy, because some strain relaxation is allowed which is not possible in a thin film, but it also results in an increase in the surface energy. This means that there is an island size at which the total energy is minimized.

It is now well established that many combinations of semiconductors grow in the Stranski–Krastanow mode, and this can be utilized for the self-assembly of quantum dots. The most studied example is InAs on GaAs where high quality quantum dots can be grown with both molecular-beam epitaxy (MBE) and metal–organic vapour-phase epitaxy. Dots form at a critical thickness of 1.5 monolayers, corresponding to just 4 Å of material [9]. For thicknesses less than the critical thickness, the covering is not completely uniform; there are island-like structures, elongated along the $[0\bar{1}1]$ direction. However, at the critical thickness, dots form, leaving a thin InAs layer, the wetting layer, between the dots. As more InAs is added, the density of dots increases with only small changes in the dot size. As an example, figure 2 shows the topography of InAs dots on a GaAs substrate measured with an atomic force microscope. The dots are roughly 6 nm high and 20 nm in diameter with a density of 10^{10} cm^{-2}.

The dots grown in the Stranski–Krastanow mode are free of dislocations, which is an essential prerequisite in III–V compounds for a high quantum efficiency for optical emission. Furthermore, the dots are remarkably homogeneous. Statistical fluctuations during growth will always give rise to a distribution in dot size, height and composition. Nevertheless, the fluctuations in dot size can be as small as about 10% [9]. The dots are randomly arranged in the lateral plane if the growth proceeds on a flat substrate, and densities lie typically between 10^9 and 10^{11} cm^{-2}. The shape and composition of the dots depend on the growth parameters. For instance, InAs/GaAs dots can have facets along particular crystal directions, or they can be lens-shaped without facets, depending on the growth technique, and in particular the growth temperature.

Stranski–Krastanow growth has turned out to be a robust phenomenon for semiconductor materials; quantum dots have been produced in this way for a number of material combinations. The most important condition is that the deposited material has a substantially larger lattice constant than does the substrate. InAs forms dots not just on GaAs but also on InP. The InAs/InP dots are particularly interesting because they emit close to the technologically important 1.5 μm wavelength [10]. InP can also form the dot material by using $Ga_xIn_{1-x}P$ substrates where the bandgap is pushed up into the red region of the spectrum [11]. Dots can also be grown with II–VI materials, the growth of CdSe on ZnSe is analogous to the growth of InAs on GaAs [12]. These II–VI dots emit in the green. Finally, dots can also be formed in the nitrides, for instance by depositing $In_xGa_{1-x}N$ on an $Al_yGa_{1-y}N$ surface. In fact, the high emission efficiency of GaN, despite the large defect density, has been attributed to the formation of quantum dot-like structures in the active layers [13].

It is a challenge to arrange the dots in the plane of the substrate. An easy route with self-assembly has not been found to accomplish this. Nevertheless, dots can be encouraged to grow at particular positions by pre-patterning the substrate. This obviously limits the separation of the dots in any such array to the limits set by lithography. However, self-assembly does provide a means to order the dots in the growth direction: if the separation between successive layers is small enough (less than 15 nm for InAs/GaAs), then the dots grow directly above one another [14], as shown in figure 3. In a new layer, the residual strain field from the dots in the layer below is sufficient to seed the dots. In this way, vertical stacks of dots can be built up. In fact, it has been observed that the dots tend to become more laterally ordered with each layer [15]. The point is that, if two dots are close together in one layer, their strain fields overlap and provide only one seeding centre in the subsequent layer.

It is also a challenge to characterize the shape and composition of self-assembled quantum dots. The shape is accessible with an atomic force microscope, but only when the dots are on the surface. For all optical experiments, the dots need to be covered with the host semiconductor, otherwise the surface electric field ionizes the electron–hole pairs, rendering the material incapable of emitting light. Atomic force microscopy is unfortunately unable to provide any information on covered dots. It is only recently that significant success has been achieved with other techniques. A notable experiment is cross-sectional scanning tunnelling microscopy where the sample is cleaved in the chamber of a ultrahigh-vacuum scanning tunnelling microscope. The tunnelling current is dependent on the local composition. For InAs dots on GaAs this has led to the observation of a strong composition profile: the dots are indium rich at the top, and indium poor at the bottom [16]. While the dot in this particular experiment takes on the shape of a truncated pyramid, the region of high indium concentration is an inverted pyramid. This is a surprising result, and it is not yet clear whether this is true also for other quantum dot systems. Grazing incidence X-ray studies support the conclusion of an indium-rich apex and an indium-poor base although these measurements were performed on uncapped lens-shaped InAs dots [17]. The truncation of the pyramid is thought to take place during capping, and shape changes during capping have been directly observed in the growth of geranium dots on silicon using an *in-situ* low energy electron microscope [18].

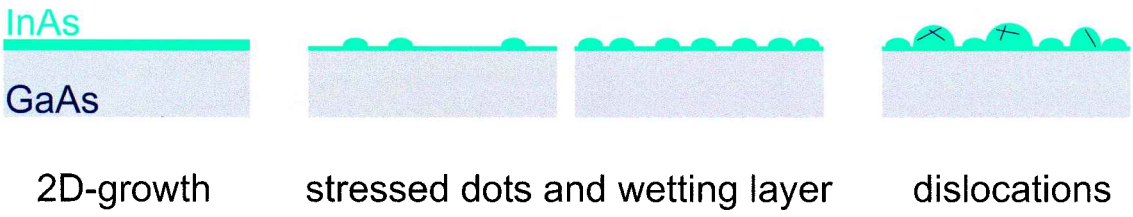

Figure 1. A schematic diagram of the Stranski–Krastanow mode. ML stands for monolayer, and the layer thickness in MLs one would have if the growth proceeded layer by layer is used as a measure of the material deposited. The material deposited has a substantially larger lattice constant than the substrate, for example InAs on GaAs. Initially, a thin and uniform layer is deposited. At the critical thickness (1.5 ML for InAs on GaAs), islands spontaneously form. Further growth results in an increase in the number of islands. At large coverages, large and dislocated islands appear.

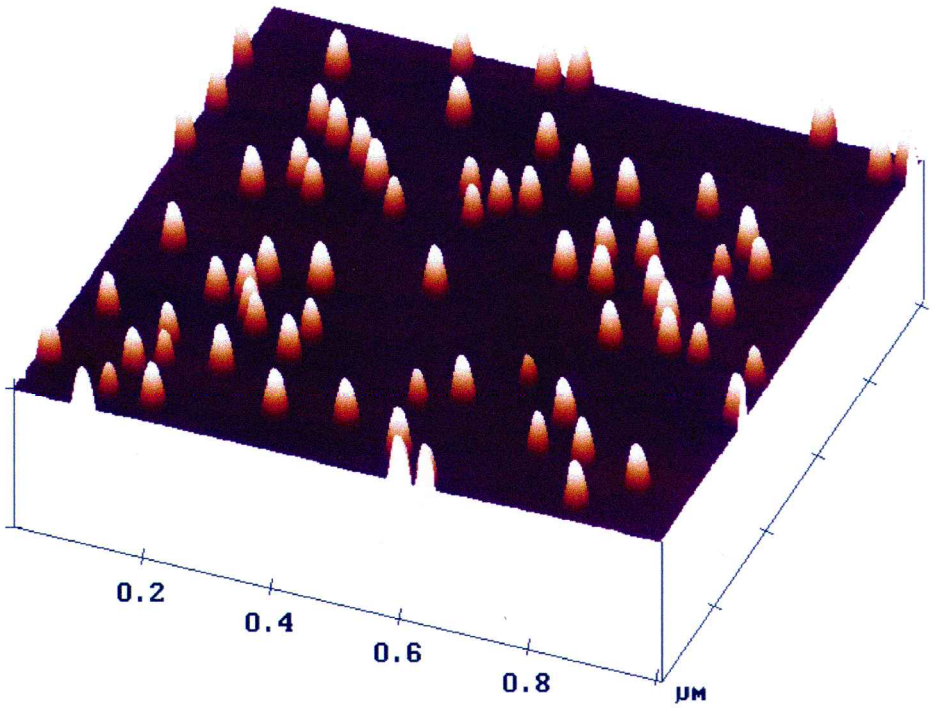

Figure 2. An atomic force micrograph of InAs quantum dots on a GaAs substrate. The InAs dots were grown by MBE at a growth temperature of 530°C. The vertical scale is expanded relative to the horizontal scale. The image was taken by Axel Lorke.

It should be noted that the self-assembly of semiconductors is a complex process, being determined largely by kinetic factors rather than by the condition for thermal equilibrium. It is now clear that the properties depend on the exact growth conditions. There are very challenging issues here, and significant progress can be anticipated through the use of growth chambers with *in-situ* structural analysis. It will also be possible to exploit the complexity to grow dots with particular properties. The extent to which this is possible is largely unknown at present.

4. Optical properties of quantum dots

The main interest in quantum dot physics is the quantization in all three spatial directions, giving rise to atomic-like energy levels. For a system of self-assembled quantum dots, it is possible to measure the fundamental bandgap, the energy separation between the confined states both for electrons and for holes, the barriers to the electron continuum and hole continuum, and the oscillator strengths for the various interband transitions with optical spectroscopy.

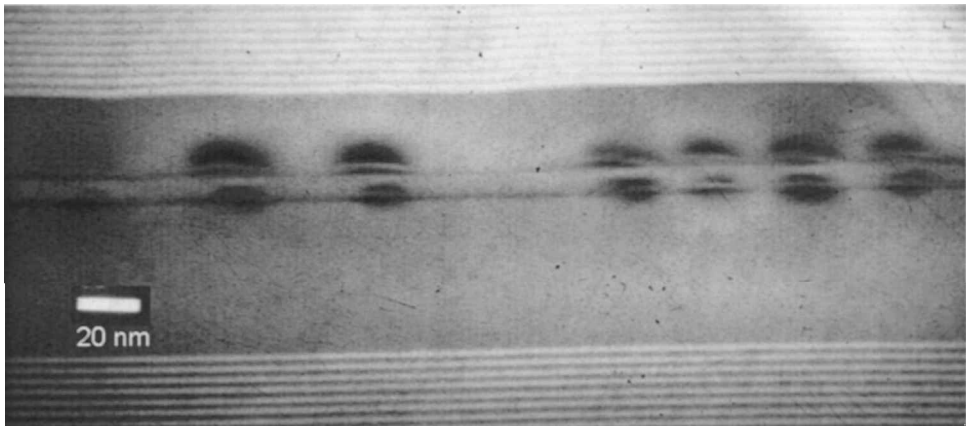

Figure 3. A cross-sectional transmission electron micrograph of two layers of InAs quantum dots in GaAs showing how the dots in the upper layer lie directly above the dots in the first. The image was taken by Gio Medeiros-Ribeiro.

Perhaps the simplest experiment to perform, if not to understand, is photoluminescence in which electron–hole pairs are excited with a laser beam, and the light re-emitted by the sample is detected. The laser energy can be tuned to lie just above the bandgap of the wetting layer in which case the electron–hole pairs are excited in the wetting layer itself. Alternatively, if the laser energy is larger than the bandgap of the barrier material, electron–hole pairs are excited also in the barrier. In both cases, the carriers relax into the dots, and then down the ladder of states in the dot, so that the dot electron and hole ground states are occupied. Light is emitted when an electron and a hole recombine. As such, the experiment measures only the energy of the ground-state exciton. However, if the pump intensity is increased such that electron–hole pairs are generated more rapidly than they can recombine, the excited states of the dots are also occupied and recombination can also occur from excited states [19, 20]. An example of such an experiment is shown in figure 4. At low pump powers, only the ground state emission is detected; at higher pump powers, the first excited state emerges and, at higher powers still, the second excited state also emerges, and so on. Photoluminescence spectra are broadened by the inhomogeneous broadening, that is fluctuations from dot to dot, but the broadening is small enough that in the experiment of figure 4 the excited state emission can be easily distinguished from the ground state emission. For these particular quantum dots, the energy separation between the ground- and excited-state emission is 15 meV, and this corresponds to the sum of the electron and hole confinement energies. The separation between the other emissions is also about 15 meV, implying that the states are approximately equally spaced, implying in turn that the confining potential is approximately parabolic. Furthermore in this experiment, emission from the wetting layer can also be seen, and this enables the depth of the electron and hole confining potentials to be estimated.

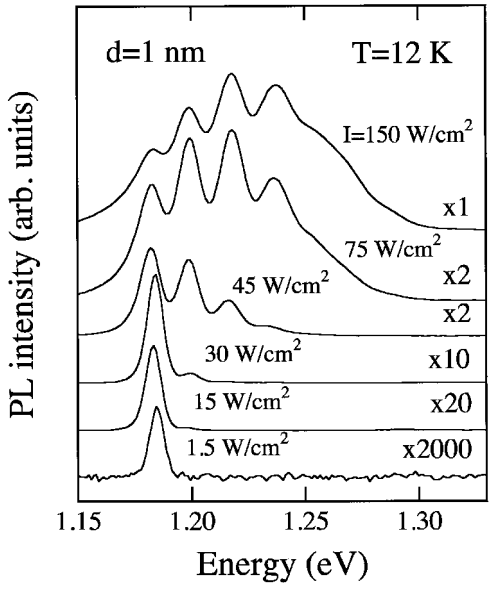

Figure 4. Photoluminescence (PL) from an ensemble of quantum dots as a function of laser excitation power. The measurement temperature was 12 K. The quantum dots are induced in an $In_xGa_{1-x}As/GaAs$ quantum well by a strain field generated by InP stressors on the sample surface. The stressors are grown in the Stranski–Krastanow mode and are 1 nm away from the quantum well. At low excitation power, only the ground state emission is observed. As the power increases, emission from excited states is also observed through state filling. The spectra at different powers are offset vertically for clarity, and the vertical scale has been magnified by the factors given ($\times 2000$, $\times 20$, $\times 10$, etc.) (Reprinted with permission from Lipsanen *et al.* [19]. Copyright 1995 American Physical Society.)

Photoluminescence invariably yields the sum of electron and hole energies. In order to measure just the electronic

properties independent of the holes, it is possible to occupy the dots with, say, two electrons (so that in each dot the twofold degenerate ground state is fully occupied) and to excite electric dipole transitions between the electron levels. This has been accomplished with so-called charge-tuneable heterostructures, with which electrons can be controllably loaded into the dots from an electron reservoir [21]. It has also been accomplished with permanently n-doped samples [22]. The interlevel absorption lies in the far infrared region of the spectrum; for InAs/GaAs quantum dots for instance, the transition is at a wavelength of 25 μm (an energy of 50 meV) [22, 23], as shown in figure 5. The results of this experiment also point to an approximately parabolic confining potential from the fact that as additional electrons are added to the dots, the energy of the far infrared absorption does not change much. (In the limit of a perfect parabolic potential, a famous result known as the generalized Kohn theorem states that the long-wavelength absorption should show no energy dependence on the electron occupation [24].)

In self-assembled quantum dots, the confining potential can be thought of as very steep in the growth direction, and relatively shallow in the lateral plane. In other words, the dots are essentially two-dimensional discs. The electron ground state is, in analogy with atomic physics, s-like, and the excited state p-like. However, because of the disc-like nature of the dots, the p-state is fourfold degenerate, and not sixfold degenerate as in a conventional atom. One way to demonstrate this is to perform interband absorption experiments on charge-tuneable structures [25], as shown in figure 6. The first transition corresponds to the transition from the hole s-state to the electron s-state, and disappears when the dots are occupied with two electrons. This is simply because the Pauli principle forbids the transition once the final level is fully occupied. The second transition corresponds to the transition from the hole p-state to the electron p-state and disappears when the dots are occupied with four electrons, confirming the degeneracies of the confined states. This experiment, unlike a photoluminescence experiment, also yields a value for the oscillator strength [25]. The result can be understood simply in terms of the overlap integral between the hole and electron states. In other words, these dots are in the so-called strong-

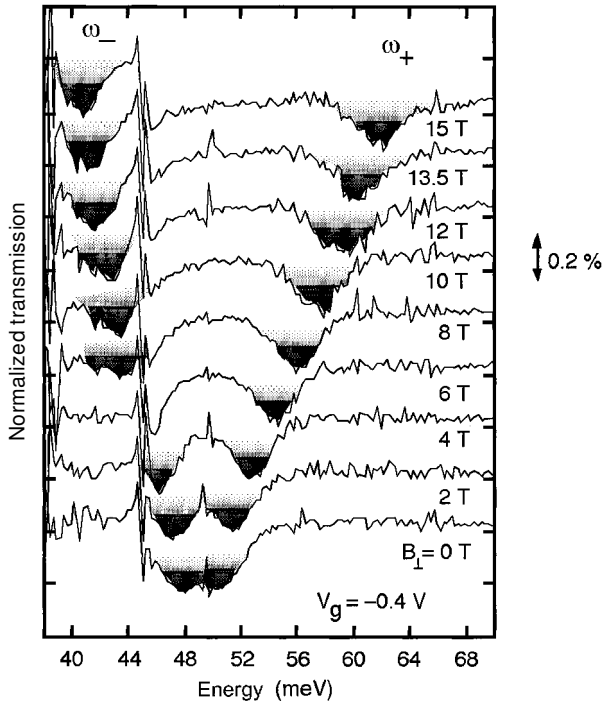

Figure 5. Transmission in the far infrared of an ensemble of InAs/GaAs quantum dots where each quantum dot is occupied with two electrons. The data were taken at a temperature of 4.2 K for a range of magnetic fields, and the spectra have been shifted vertically for clarity. The shaded transmission minima correspond to absorption from the quantum dots. The transitions are between the electron ground state and the first excited state. Two absorption peaks are observed even at zero magnetic field, suggesting that the dots are slightly oval in shape. In a magnetic field, the two peaks move apart, which is a consequence of the Zeeman effect. The strong feature at 45 meV arises from an electronic interaction with an interface phonon. (Reprinted with permission from Fricke *et al.* [23]. Copyright 1996 European Physical Society.)

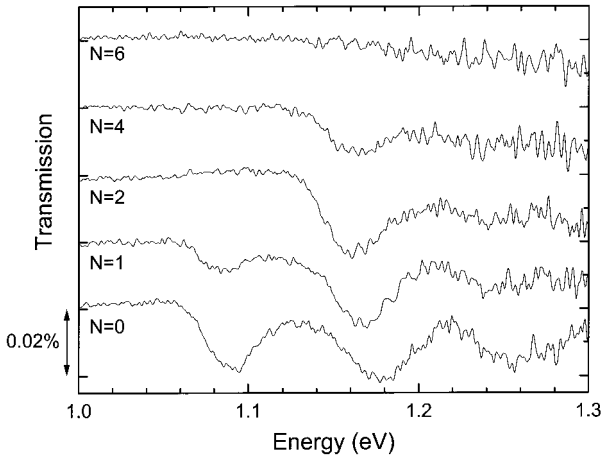

Figure 6. Transmission in the near infrared of an ensemble of InAs/GaAs quantum dots at 4.2 K. Spectra are shown for different values of N, the electron occupation. At $N = 0$, there are three transitions corresponding to transitions from a valence state to an electron state. These are the s–s, p–p and d–d transitions, where the states are labelled in analogy to atomic physics. At $N = 2$, the electron ground state is fully occupied, and the s–s transition disappears because it is blocked, a consequence of the Pauli principle. Similarly, the p–p transition is blocked at $N = 6$ when both the s and the p states of the electron are fully occupied. (Reprinted with permission from Warburton *et al.* [25]. Copyright 1997 American Physical Society.)

confinement regime where the confinement energies are larger than the exciton binding energy. In the other limit, the weak-confinement regime, the exciton binding energy dominates over the confinement energies, and it makes sense only in this limit to think of an exciton moving as a coherent entity throughout the dot. In the weak-confinement regime, the oscillator strength is actually larger than in the strong-confinement regime [26].

An important issue in interpreting photoluminescence experiments, relevant also for devices such as the quantum dot laser, is the rate at which a highly excited electron–hole pair can relax to the ground state of a quantum dot. Relaxation in the continuum is known to occur on a picosecond time scale: electrons and holes relax by emitting longitudinal optical (LO) phonons if possible and, if not, acoustic phonons, and if there are many carriers, thermal equilibrium is established in both conduction and valence bands through carrier–carrier scattering. Capture of carriers into a quantum dot from the continuum also occurs quickly (apart from in low-density samples where capture may take a few hundred picoseconds). It was initially thought that relaxation of carriers once captured by a quantum dot would be hindered by the discrete nature of the density of states [27]. The argument is that the energy separation between the levels is too large for efficient acoustic phonon emission; and there is no reason why the separation between the levels should match the LO phonon energy (which has a very weak dispersion). Nonetheless, experiments have shown that relaxation from excited dot states to the ground state is rapid, occurring on a picosecond-time scale [28, 29], very nearly as for quantum wells. There are a number of explanations for the absence of the 'phonon bottleneck'. First, an electron in an excited state may relax to the ground state by scattering off a hole in the same dot, with the hole then relaxing by phonon emission [29]. The importance of this mechanism depends on the large hole effective mass, which gives rise to a large number of closely spaced hole levels, and also a strong coupling to the phonons, allowing efficient hole relaxation. Secondly, Auger processes are possible when the sample is highly excited; an electron in a dot loses energy by promoting an electron in the continuum to a higher energy. Thirdly, it has been suggested that the dot itself influences the phonon spectrum such that a LO phonon can decay into acoustic phonons quite rapidly, broadening the LO phonon spectrum, and allowing fast relaxation by LO phonon emission over a range of energies tens of millielectronvolts wide [30]. Despite this latter prediction, there is some evidence for phonon bottleneck for quantum dots occupied with just one electron without a hole, and without a population in the wetting layer [31]. Under less extreme conditions, however, it is now clear that relaxation occurs more rapidly than recombination (the recombination time is typically 1 ns for self-assembled quantum dots), just as for quantum wells. This is a useful property for interband lasers, but a difficulty for potential interlevel lasers where it would be extremely desirable to decrease the relaxation rate.

5. Single-dot spectroscopy

There are inevitably fluctuations in both size and composition from one dot to the next, and this leads to inhomogeneously broadened transitions in optical spectroscopy. For self-assembled InAs dots on GaAs, the lowest linewidth of the photoluminescence from a weakly excited ensemble of dots is at present about 20 meV. Obviously, this width can be much larger for highly inhomogeneous samples. The inhomogeneous broadening is large compared with other relevant energies. For instance, the emission from a biexciton (a complex of two excitons) or charged exciton (a complex of an exciton and one additional electron) is typically shifted by a few millielectronvolts from the emission of a neutral exciton. It is difficult to resolve these shifts clearly with an experiment on an ensemble. A further energy scale is the homogeneous width which, although as yet unexplored in any great detail, can be as small as a few microelectronvolts [28]. In order to access these effects on a milliectronvolt or sub-millielectronvolt energy scale, it is necessary to perform optical experiments on single quantum dots rather than ensembles. The development of this field has been aided by the techniques developed for single-molecule spectroscopy which was first reported in the late 1980s and has subsequently become a routine, if challenging, experimental technique [32].

Single-molecule spectroscopy is usually performed by spinning a suspension of molecules on to a substrate such that the molecules are separated by several microns. A molecule is excited by a focused laser beam, with the same lens collecting also its emission. With a high numerical aperture lens, only the emission from one molecule is collected. A confocal arrangement, with a pinhole as a spatial filter, can increase the signal-to-noise ratio by rejecting all light originating from outside the focus. The same technique can also be used for single quantum dot spectroscopy, provided that the dot density is low enough so that there is only ever one dot in the focus. While samples with a low density have been produced for single dot experiments, usual samples have a larger dot density, 10^{10} cm^{-2} being typical. This density translates into 100 dots μm^2, the area of the spot size in a good microscope, and in this case the smooth ensemble emission spectrum breaks up into overlapping sharp lines, as shown in figure 7. This is a strong indication that individual dots give sharp emission lines, but it is difficult to perform detailed experiments when the lines cannot be spectrally distinguished.

Given that the spot size of a confocal microscope is in the best case diffraction limited, it is clear that conventional

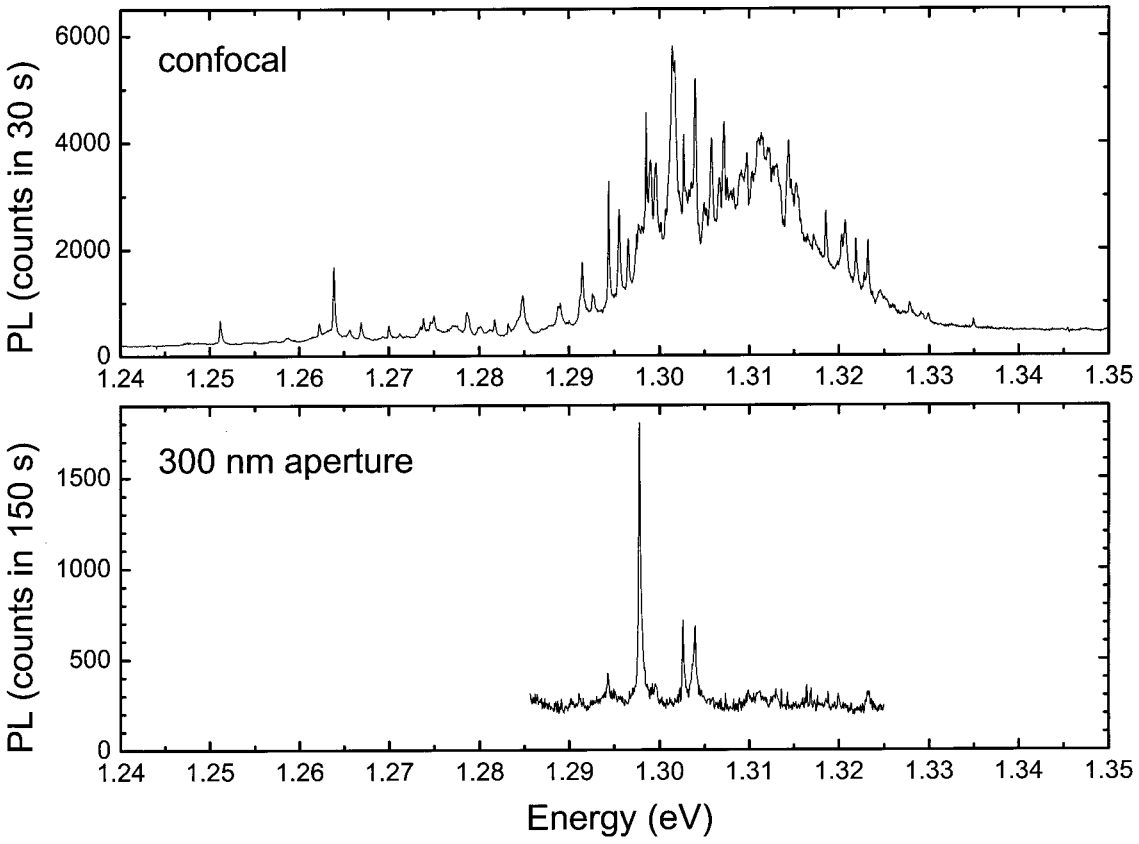

Figure 7. Emission from quantum dots (*a*) from a 1 μm^2 area of the sample and (*b*) from a 0.07 μm^2 area of the sample, both taken at 4.2 K. The quantum dots are generated with Stranski–Krastanow growth of InAs on GaAs, using an annealing step to increase the photoluminescence (PL) energy from about 1.1 eV to about 1.3 eV. The spectrum in (*a*) was taken with a low temperature confocal microscope; and the spectrum in (*b*) with a near-field technique. It can be seen how large statistical fluctuations arise in the spectrum in (*a*), because the number of rings probed is not sufficient to give a smooth distribution function. In the spectrum in (*b*) just a few peaks can be discerned above the noise level, each arising from the emission from an individual quantum dot.

far-field optics will not provide the spatial resolution to probe unambiguously just one dot. The diffraction limit can be bypassed by a near-field technique in which a subwavelength-sized aperture is positioned in close proximity to the sample. In this case, the aperture size determines the spatial resolution, not the wavelength of light, but there is inevitably a large reduction in the signal strength. One implementation of this idea is to use a tapered metallized optical fibre as a probe, brought controllably to within a few nanometres of the sample surface [33]. Another method is to define lithographically nanometre-sized apertures in a metallic layer deposited on the sample [34]. This is simpler than the use of the tapered fibre but has the disadvantage that the aperture cannot be moved with respect to the sample, prohibiting any imaging, but at least many apertures can be defined in one sample, allowing a large number of individual dots to be addressed. A further technique is to etch subwavelength-sized pillars in the sample, such that each pillar contains on average about one quantum dot [35]. A possible problem here is the effect of the free surface on the quantum dots' optical properties. Many of the experiments on single dots need to be carried out at a low temperature and both miniature optical cryostats [35, 36] and top-loading bath cryostats [37] have been used.

The photoluminescence signal from a single quantum dot in a near-field experiment can be very small, possibly just a few hundred photons per second, and a single-photon detector with a high quantum efficiency and low dark count is essential. A cooled silicon charge-coupled device (CCD) camera is extremely convenient, offering in addition to its high detectivity an invaluable multiplexing advantage. However, the response of a silicon camera tails off in the visible, and decreases rapidly for wavelengths longer than 1050 nm; so it is by no means a universal solution. In fact most of the single dot experiments on InAs-based systems have used quantum dots with some gallium incorporation in order to push

the bandgap up so that the emission can be detected with a silicon camera.

The most striking property of the emission from a single quantum dot at low temperature is its spectral purity [38, 39]. Linewidths as small as 25 μeV, corresponding to 6.0 GHz, have been reported for quantum dots formed in localizing potentials in a quantum well [28]. The exact line widths of self-assembled quantum dots are difficult to measure because they are smaller than the spectral resolution of grating spectrometer–CCD array systems. The linewidth is a measure of the exciton dephasing time which is at most the radiative lifetime. This limit of lifetime broadening has been observed at low temperature on natural quantum dots but, as the temperature increases, the linewidth increases because of scattering by acoustic phonons [28]. It remains to be seen what the corresponding behaviour is for self-assembled dots. The homogeneous width is clearly important for futuristic applications of quantum dots as the elements for quantum information processing, as it is essential that the system maintains its phase coherence during the manipulation of the quantum mechanical wavefunctions.

The sharp lines in single dot spectroscopy give access to the rich physics on a millielectronvolt energy scale for quantum dots. This includes small energy shifts through the Coulomb interaction. When a quantum dot containing several excitons decays, the photon energy is renormalized by the Coulomb interactions between the electrons and holes such that the train of photons emitted when a highly excited dot decays all have different energies [35]. Alternatively, a quantum dot can be occupied with a known number of electrons by designing a suitable voltage-tuneable heterostructure [25]. Every time that an electron is added to the dot, the emission red shifts, and the size of the shift reveals a shell structure [37, 40]: whenever an electron can be added with the benefit of exchange energy, the shift in the emission is small but, whenever an electron is added to complete a subshell, the shift in the emission is relatively large. Notably, the emission for a doubly charged exciton splits into two, a triplet and a singlet, as shown in figure 8. This is because the two electrons in the final state, after the emission of a photon, have either parallel or antiparallel spins, configurations with different energies because of the exchange interaction. This is entirely analogous to the excited state of the helium atom: the splitting of the lines of the doubly charged exciton is simply twice the exchange energy.

6. Colloidal quantum dots

The focus of this article is the properties of quantum dots which are self-assembled in the growth of inorganic semiconductors on planar substrates. However, rapid progress has been made in the last decade in fabricating inorganic quantum dots with techniques from organic chemistry [41, 42]. The end result is a suspension of quantum dots in an organic, or even aqueous, solution.

There are a number of ways to prepare semiconductor nanocrystals in a chemical solution, most of which rely on fast nucleation followed by relatively slow growth [42]. If the growth proceeds smoothly, a particular crystal size can be obtained simply by stopping the growth after a certain time. One important method is to mix a methyl metal alkyl (e.g. dimethylcadmium) and a chalcogen source (e.g. tri-*n*-octylphosphine selenide) in tri-*n*-octylphosphine (TOP). The mixture is then injected into hot tri-*n*-octylphosphine oxide (TOPO) [43]. The temperature, up to about 350°C, is high enough for nanocrystals to nucleate (CdSe in this example). The nanocrystals are crystalline and can be made with diameters of between about 2 and 20 nm with a size inhomogeneity of about 5%. This method requires injecting metal alkyls at elevated temperatures and is potentially hazardous. It has been shown, however, that this problem can be avoided by the use of a molecular precursor in which the metal–chalcogen bond is already in place [42].

The nanocrystals have a large proportion of their atoms close to the surface, meaning that the surface plays a very important role. A crucial aspect of these techniques is that the surface is passivated by a monolayer of the solvent ligands, as shown schematically in figure 9, such that the quantum efficiency for optical emission can be as high as 10%. By way of comparison, commercial dye molecules have quantum efficiencies between 12% and 70%. Without this passivation, the nanocrystal quantum efficiency would be extremely low. The quantum efficiency can be increased further, up to 50%, by designing a so-called core–shell structure; the core is coated with a semiconductor with a larger bandgap, which limits the influence of the surface by confining the carriers to the core region. An example of a core–shell structure is the CdSe/CdS system.

It is easiest to grow II–VI semiconductor nanocrystals in this way. III–V semiconductors are more covalent in character and this means that crystal formation is hampered by large energy barriers. Nevertheless, III–V nanocrystals have been produced by using appropriate precursors [42].

Quantum confinement effects are particularly striking in these materials. With just one material, a wide range of emission energies is possible simply by varying the size of the nanocrystals. By additionally using different materials, emission over a wide band of wavelengths can be demonstrated, as shown in figure 10. This has been extended into the infrared recently, to the all important 1.5 μm telecommunications wavelength, by developing techniques for self-assembling CdTe/HgTe quantum dots [44].

There are several possible applications of this technology. One is the use of water-soluble nanocrystals for biological labelling where a number of different labels can

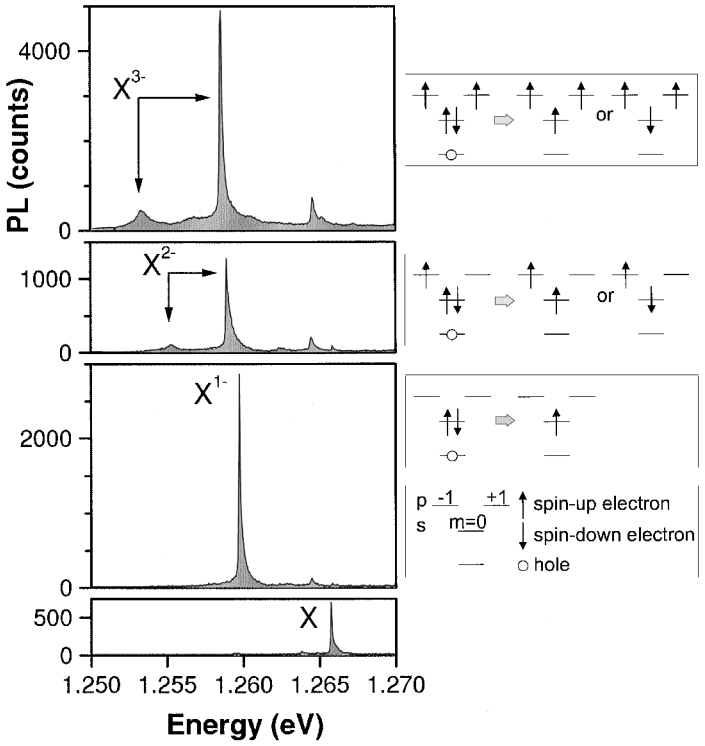

Figure 8. Photoluminescence (PL) emission spectra from a single quantum dot as a function of charge. X is the neutral exciton, X^{1-}, the singly charged exciton, X^{2-} the doubly charged exciton, and X^{3-} the triply charged exciton. The level diagram shows the hole ground state, the electron ground state and the electron excited state. The states are labelled s and p, and the *z*-component of angular momentum *m* as in atomic physics. The hole is shown as an open circle, and electrons as ↑ and ↓ depending on the spin. Each time that an additional electron is added, the emission shifts to the red. In addition, for the X^{2-}, there are two emission lines because there are two possible final states, as shown in the level diagrams, with different energies because of the exchange interaction.

be employed, each identifiable by the wavelength of the emission [45]. An advantage of the nanocrystals over conventional dye molecules is that all nanocrystals can be excited more or less equally with a short-wavelength source. The nanocrystals may also find application in optoelectronic devices, such as solar cells. There are, however, serious challenges to be met in this field. The nanocrystals tend to lose their advantageous optical properties in the course of time. For instance, TOPO-capped II–VI materials degrade in the presence of light and oxygen: unstable chalcogen oxides form. The nanocrystals also photobleach; the emission from individual nanocrystals turns on and off randomly, even with uniform cw excitation. Even in the on periods, the emission from nanocrystals exhibits temporal wanderings in wavelength [46]. These effects are related to the localization of charge at defects on the surface. In other words, the deleterious effects of the surface have not been eliminated entirely. Also, there are important issues in how to embed the nanocrystals into devices. However, progress can be expected in all these areas, and these nanocrystals represent a fascinating approach to building novel photonics devices.

7. Applications of quantum dots

Quantum dots are potentially useful for a number of different technologies. While there is at present no established application of quantum dots, there are a number of very promising areas.

7.1. *Laser diodes*

The development of laser diodes over the past three decades has been a success story. Through improvements in material quality and processing techniques, the threshold currents have gradually decreased. Significantly, a reduction in the effective dimensionality of the active layer, from three to two, has made a considerable improvement. This is related to the density of states. In a three-dimensional band structure, the density-of-states increases with energy E (as $E^{1/2}$ close to the band edge at $E=0$), and this limits gain at the lasing wavelength; the available carriers are spread over a narrow band of energy, limiting the population inversion at the lasing wavelength because of the finite temperature. In a quantum well, the density of states for each quantized level (or subband) is constant, so that the same number of

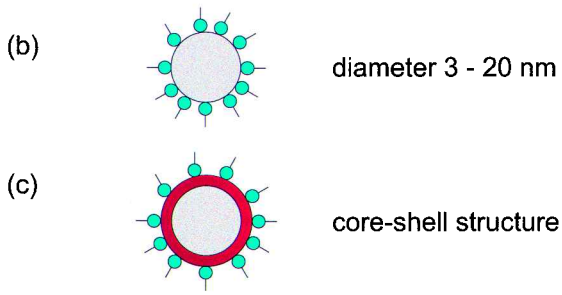

Figure 9. (*a*) A schematic diagram of the growth of semiconductor nanocrystals; (*b*) the surface passivation with ligands; (*c*) a core–shell structure.

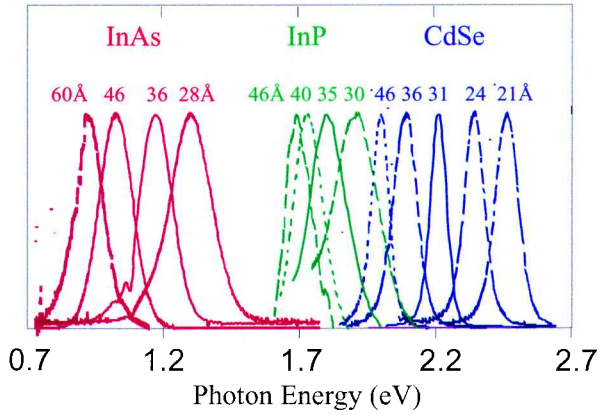

Figure 10. Room-temperature emission spectra of surfactant-coated colloidal quantum dots. The blue series are CdSe nanocrystals, the green series are InP nanocrystals, and the red series InAs nanocrystals. Selection of the size (60 Å, 46 Å, 36 Å, 28 Å, etc.) has been used to give a particular wavelength in each band. (After [44]. Reprinted (abstracted/excerpted) with permission from Bruchez *et al.* [44]. Copyright 1998 American Association for the Advancement of Science.)

carriers are spread over a much larger energy than in the three-dimensional case, increasing the gain at the lasing wavelength. An additional improvement can be obtained by confining not only the electrons and holes but also the light. To do this, a waveguide structure is incorporated into the heterostructure by exploiting the small refractive indices of wide gap compounds. This confines the light along the growth direction. Light confinement is also possible in the lateral directions by post-growth processing steps, for instance the etching of a ridge mesa.

The fundamental laser characteristic is the threshold current, the current at which optical transparency is achieved, such that at currents higher than the threshold current there is net gain and lasing occurs. Typically, the threshold current depends exponentially on the temperature, $I = I_0\ \mathrm{e}^{T/T_0}$, where T is the temperature, T_0 is the characteristic temperature and I_0 is the low-temperature threshold current. Ideally, a laser has a small I_0 and a high T_0. However, in many contemporary applications of semiconductor laser diodes, the crucial quantity is the maximum modulation frequency as this determines the bit rate for data transmission through optical fibres. As can be shown by a rate equation analysis, the bandwidth is high in the case of high gain.

A semiconductor laser diode with a large density of perfect quantum dots is predicted to have optimum properties: a low and temperature-insensitive threshold current and a large modulation bandwidth [47]. 'Perfect' in this context implies that the dots have very deep confinement potentials (on the scale of the thermal energy, 25 meV at room temperature) and that they are all identical. Again, the fundamental reason for this is related to the density of states. For a homogeneous ensemble of quantum dots, the density of states is a sharp peak at the interband transition energy. For each dot, only two electrons must be excited across the gap to establish population inversion. This is also true at high temperature for a deep confinement potential. All this leads to the attractive properties, and these predictions have motivated much of the recent work on quantum dot lasers.

In practice, self-assembled quantum dots are not perfect for application as the gain medium in a laser diode. A number of issues arise. First, the dots are inhomogeneous so that only a fraction of the dots can contribute to the lasing signal; the majority are inverted uselessly. This corresponds to a penalty on the threshold current. Second, the dot densities are typically about $10^{11}\ \mathrm{cm}^{-2}$ for these applications, implying that in the layer plane there is more unoccupied space than dot material. This limits the material gain. Third, the dots do not have deep enough confinement potentials; carriers thermally populate excited dot states, and they can also escape out of the dot before contributing to stimulated emission. Finally, the carriers are electrically injected and must diffuse laterally into the quantum dots, and this can cause gain saturation at modest currents. It is therefore not obvious whether the inherent advantages of quantum dots can be exploited with self-assembled techniques.

Quantum dot lasers have now been realized and emit a continuous wave at room temperature, and the properties of the diodes have already improved significantly since the first reports of laser action [48]. Low temperature thresholds have been reported which compare very favourably with the best quantum well laser diodes [48]. At low

temperatures, T_0 can be as high as 385 K, and this is clearly a consequence of the carrier confinement in the quantum dots [49]. However, at room temperature it is fair to say that the dream of an ultrahigh T_0 has not been realized: T_0 decreases rapidly above, say, 300 K, causing the threshold current to increase markedly.

Even if the intrinsic advantages of quantum dots are at present offset by the inhomogeneous broadening for laser applications, quantum dot lasers already offer some other advantages over conventional laser diodes. The InAs/GaAs quantum dot emission wavelength is significantly higher than that of $In_xGa_{1-x}As/GaAs$ quantum wells, and with subtle changes in the growth can be increased to 1.3 μm, corresponding to one of the low-loss windows in optical fibre. Lasers emitting at this wavelength are typically fabricated with inferior InP-based technology. Also, much higher powers have been realized with quantum dot lasers than with quantum well lasers. In quantum well lasers, device failure occurs at high currents, often owing to degradation of the end mirrors. It would appear that the carrier localization in quantum dots is sufficiently strong to prevent diffusion to the end facets, allowing the devices to withstand higher currents.

7.2. *Single-photon sources*

There is a pressing need in quantum cryptography for a single photon source. Quantum cryptography uses either the phase or the polarization of single photons as the means of communication and can achieve almost totally secure transmission [50]. The basic idea is that the sender rotates his or her basis randomly, making it impossible for an eavesdropper to detect a photon and accurately to recreate it. For this technology to become viable, a single photon emitter is required. In prototype systems, a highly attenuated laser pulse is used as the source, but this is both inefficient as the majority of pulses are empty, and insecure, as a sizeable fraction of the pulses contain two photons. A source consisting of a single quantum dot can in principle overcome these limitations. The advantage of quantum dots over single molecules for these applications is that quantum dots, unlike single molecules, do not suffer from photobleaching, although progress has recently been made in the preparation of single molecules by embedding terrylene molecules in a *p*-terphenyl molecular crystal [51]. A powerful idea in quantum dot physics is to excite a quantum dot with a laser pulse intense enough that the probability of the dot capturing at least one exciton is very close to one [52]. A highly excited quantum dot decays by emitting a series of photons, which have different energies because of the renormalization through the Coulomb interaction. This enables the final photon to be selected by spectral filtering, and this photon can be used for communication.

This idea has now been explored experimentally and, at least at low temperatures, photons on demand have been generated from individual quantum dots [53, 54]. This is often called non-classical light because the temporal ordering of the photons is highly dissimilar from classical light described by Poisson statistics.

Quantum dots emit photons in all possible directions so that only a fraction of the emitted photons can ever be collected and subsequently detected. In a single dot experiment, this limits the signal-to-noise ratio and, in a realization of quantum cryptography, it seriously limits the bit rate. One solution to this problem is to place a quantum dot in a microcavity tuned to the emission of the quantum dot. The cavity changes the photon density of states. At resonance, this increases the radiative decay rate and it also forces the photons to be emitted into the cavity modes. The cavity modes are controllable and therefore allow in principle a much increased detection efficiency. The increase in radiative decay rate, known as the Purcell effect, has been experimentally observed by monitoring the temporal decay of excitons in quantum dots placed in a Fabry–Pérot etalon [55]. The two mirrors of the etalon are formed from Bragg reflectors in the heterostructure itself and consist of a stack of AlAs/GaAs pairs, with each layer of optical thickness $\lambda/4$. The two mirrors define a microcavity in the vertical direction; to confine the optical mode also in the lateral direction, a pillar is etched through the entire structure with a diameter of about a micrometer. The decay rate has been increased by a factor of 5 with this technique, with a concomitant change in the spatial distribution of the emission. So far, this remains a low temperature effect; at high temperatures the quantum dot emission is significantly broadened such that a matching cavity has a low quality factor, giving a weak Purcell effect.

7.3. *Other possible applications*

An individual quantum dot has the capability of trapping individual electrons or holes and it might be possible to exploit this as a memory element with a bit represented by a single electron in a single quantum dot. For this to succeed, it is necessary that the storage time is long enough to be practical. One of the most important parameters is the height of the energy barrier ΔE separating the quantum dot level from the continuum at higher energies. For $\Delta E \gg k_B T$, the thermal escape rate is small; in the other limit, $\Delta E \ll k_B T$, the thermal escape rate is large (k_B is the Boltzmann constant and T the temperature). For the self-assembled quantum dots in III–V semiconductors at present available, ΔE is at most a few hundred millielectronvolts, and this leads to large thermal escape rates at room temperature. However, at 77 K, the temperature of liquid nitrogen, the thermal escape rate can be much reduced. Notable here are

InAs dots on an InP substrate which have a particularly deep confining potential for holes [10], leading to almost unmeasurably small thermal emission rates at 77 K [56]. While a device architecture does not yet exist for such devices, it has been suggested that the inhomogeneity of the quantum dots could be used for storage applications, with each dot colour representing a storage possibility [57].

The basic principle of an optical quantum dot-based storage device is to separate the electron and hole in the optically excited electron–hole pair with a strong electric field. One elegant way to do this is to use vertically oriented quantum dots in a field-effect heterostructure. The electric field can be changed simply through a voltage applied to the gate electrode. On illumination (the write part of the process), a large negative bias is applied to generate a high electric field in the device. Quantum dots in one layer trap one or more electrons, and dots in the other layer one or more holes. After illumination, a positive bias is applied so that the electrons tunnel into the dots containing the holes. The electrons and holes recombine, generating light (the read step of the process). This scheme has been implemented using a layer of self-assembled quantum dots and an adjacent quantum well [58]. In this case, the residual strain field generates quantum dots in the quantum well through the effects of strain on the electronic band structure. Existing devices exhibit memory effects which persist up to many seconds at low temperature (10 K), but the effect disappears for temperatures above about 130 K. It is also possible to implement this idea in vertically oriented self-assembled quantum dots [59]. These experiments are interesting in the sense that they represent an approach to engineering the radiative lifetime of excitons in III–V semiconductors. For instance, a storage time of 1 s corresponds to an increase in the radiative lifetime by a factor of 10^9 beyond that of an ordinary quantum dot. The experiments demonstrate that it is possible to have both long carrier storage, for which one usually uses silicon, and efficient emission, for which silicon is unsuitable, in the same device.

An alternative approach is to detect the charge stored in a quantum dot electrically. A powerful idea is to embed the quantum dots a few tens of nanometres away from a two-dimensional electron gas [60]. For a fixed electric charge density, the resistance of the two-dimensional electron gas depends on the way that the charge is distributed. When the quantum dots are neutral, the resistance is low; when however, the quantum dots are charged, the resistance is high because the charged dots both deplete locally the two-dimensional electron gas and also act as efficient scatterers. This enables the charge state of the quantum dots to be determined through the electrical resistance of the device. The charge in the quantum dots can be altered by illumination, typically with a bias applied. A variety of device geometries are possible. For instance, on illumination with light at the dots' resonant energy, the dots can be used to store a metastable population of electrons [61]. Alternatively, the two-dimensional channel itself can be used as an absorber, in which case hole tunnelling can deplete already occupied quantum dots [62]. In the latter case, for small devices with a gate electrode 1 μm long, the resistance of the device is sensitive to individual charging events, and therefore to the detection of single photons [62]. It remains to be seen whether this technology can offer a competitive alternative to the concept of single-photon detection with avalanche photodiodes.

8. Conclusions

The self-assembly of quantum dots has revitalized the field of semiconductor heterostructures as it allows the creation of quantum objects which confine both electrons and holes in all three spatial directions. The physics of quantum dots are dominated by the confinement; in a quantum dot, the band structure of the host material breaks up into a set of discrete levels. In some ways, the dots take on the properties of atoms, but with highly unusual characteristics. However, many of the properties, for instance the relaxation of the electrons from one level to the next, are strongly influenced by the presence of the solid matrix between the dots. It is possible to embed quantum dots into complicated semiconductor heterostructures and this is facilitating detailed physics experiments and the development of novel photonic devices, such as quantum dot lasers.

References

[1] http://www.nobel.se.

[2] Kittel, C., 1995, *Introduction to Solid State Physics*, 7th edition (New York: Wiley).

[3] Bastard, G., 1988, *Wave Mechanics Applied to Semiconductor Hetersostructures* (New York: Wiley).

[4] Davies, J. H., 1998, *The Physics of Low-dimensional Semiconductors* (Cambridge University Press).

[5] von Klitzing, K., Dorda, G. and Pepper, M., 1980, *Phys. Rev. Lett.*, **45**, 494; von Klitzing, K., 1986, *Rev. Mod. Phys.*, **58**, 519.

[6] Stormer, H. L., 1999, *Rev. Mod. Phys.*, **71**, 875.

[7] Weisbuch, C. and Winter B., 1991, *Quantum Semiconductor Structures* (New York: Academic Press).

[8] Grundmann, M. and Bimberg, D. 1997, *Phys. Rev. B.*, **55**, 9740.

[9] Leonard, D., Pond, K. and Petroff, P. M., 1994, *Phys. Rev. B.*, **50**, 11 687.

[10] Pettersson, H., Warburton, R. J., Kotthaus, J. P., Carlsson, N., Seifert, W., Pistol, M. -E. and Samuelson, L., 1999, *Phys. Rev. B.*, **60**, R11 289.

[11] Carlsson, N., Seifert, W., Petersson, A., Castrillo, P., Pistol, M. E. and Samuelson, L., 1994, *Appl. Phys. Lett.*, **65**, 3093.

[12] Hommel, D., Leonardi, K., Heineke, H., Selke, H., Ohkawa, K., Gindele, F. and Woggon, U., 1997, *Phys. Stat. sol.* (b), **202**, 835.

[13] O'Donnell, K. P., Martin, R. W. and Middleton, P. G., 1999, *Phys. Rev. Lett.*, **82**, 237.

[14] Xie, Q., Madhukar, A., Chen, P. and Kobayashi, N. P., 1995, *Phys. Rev. Lett.*, **75**, 2542.

[15] Tersoff, J., Teichert, C. and Lagally, M. G., 1996, *Phys. Rev. Lett.*, **76**, 1675.
[16] Liu, N., Tersoff, J., Baklenov, O., Holmes Jr., A. L. and Shih, C. K., 2000 *Phys. Rev. Lett.*, **84**, 334 (2000).
[17] Kegel, I., Metzger, T. H., Lorke, A., Peisl, J., Stangl, J., Bauer, G., Garcia, J. M. and Petroff, P. M., 2002, *Phys. Rev. Lett.*, **85**, 1694.
[18] Sutter P. and Lagally, M. G., 1998, *Phys. Rev. Lett.*, **81**, 3471.
[19] Lipsanen, H., Sopanen, M. and Ahopelto, J., 1995, *Phys. Rev. B.*, **51**, 13 868.
[20] Raymond, S., Fafard, S., Poole, P. J., Wojs, A., Hawrylak, P., Charbonneau, S., Leonard, D., Leon, R., Petroff, P. M. and Merz, J. L., 1996, *Phys. Rev. B.*, **54**, 11548.
[21] Drexler, H., Leonard, D., Hansen, W., Kotthaus, J. P. and Petroff, P. M., 1994, *Phys. Rev. Lett.*, **73**, 2252.
[22] Hameau, S., Guldner, Y., Verzelen, O., Ferreira, R., Bastard, G., Zeman, J., Lemaitre, A. and Gérard, J. M., 1999, *Phys. Rev. Lett.*, **83**, 4152.
[23] Fricke, M., Lorke, A., Kotthaus, J. P., Medeiros-Ribeiro, G. and Petroff, P. M., 1996, *Europhys. Lett.*, **36**, 197.
[24] Brey, L., Johnson, N. F. and Halperin, B. I., 1989, *Phys. Rev. B.*, **40**, 10 647.
[25] Warburton, R. J., Dürr, C. S., Karrai, K., Kotthaus, J. P., Medeiros-Ribeiro, G. and Petroff, P. M., 1997, *Phys. Rev. Lett.*, **79**, 5282.
[26] Bryant, G. W., 1988, *Phys. Rev. B.*, **37**, 8763.
[27] Benisty, H., Sotomayor-Torres, C. M. and Weisbuch, C., 1991, *Phys. Rev. B.*, **44**, 10 945.
[28] Gammon, D., Snow, E. S., Shanabrook, B. V., Katzer, D. S. and Park, D., 1996 *Science*, **273**, 87.
[29] Sosnowski, T. S., Norris, T. B., Jiang, H., Singh, J., Kamath, K. and Bhattacharya, P., 1998, *Phys. Rev. B*, **57**, 9423.
[30] Li, X. -Q., Nakayama, H. and Arakawa, Y., 1999, *Phys. Rev. B*, **59**, 5069.
[31] Urayama, J., Norris, T. B., Singh, J. and Bhattacharya, P., 2001, *Phys. Rev. Lett.*, **86**, 4930.
[32] Weiss, S., 1999, *Science*, **283**, 1676.
[33] Obermüller, C., Deisenrieder, A., Abstreiter, G., Karrai, K., Grosse, S., Manus, S., Feldmann, J., Lipsanen, H., Sopanen, M. and Ahopelto, J., 1999, *Appl. Phys. Lett.*, **74**, 3200.
[34] Gammon, D., Snow, E. S., Shanabrook, B. V., Katzer, D. S. and Park, D., 1996, *Phys. Rev. Lett.*, **76**, 3005.
[35] Bayer, M., Stern, O., Hawrylak, P., Fafard, S. and Forchel, A., 2000, *Nature*, **405**, 923.
[36] Landin, L., Miller, M. S., Pistol, M.-E., Pryor, C. E. and Samuelson, L., 1998, *Science*, **280**, 262.
[37] Warburton, R. J., Schäflein, C., Haft, D., Bickel, F., Lorke, A., Karrai, K., Garcia, J. M., Schoenfeld, W. and Petroff, P. M., 2000, *Nature*, **405**, 926.
[38] Marzin, J.-Y., Gérard, J.-M., Izraël, A., Barrier, D. and Bastard, G., 1994, *Phys. Rev. Lett.*, **73**, 716.
[39] Grundmann, M., Christen, J., Ledontsov, N. N., Böhrer, J., Bimberg, D., Ruvimov, S. S., Werner, P., Richter, U., Gösele, U., Heydenreich, J., Ustinov, V. M., Egorov, A. Yu., Zhukov, A. E., Kop'ev, P. S. and Alferov, Zh. I., 1995, *Phys. Rev. Lett.*, **74**, 4043.
[40] Hartmann, A., Ducommun, Y., Kapon, E., Hohenester, U. and Molinari, E., 2000, *Phys. Rev. Lett.*, **84**, 5648.
[41] Gaponenko, S. V., 1998, *Optical Properties of Semiconductor Nanocrystals* (Cambridge University Press).
[42] Green M. and O'Brien, P., 1999, *Chem. Commun.*, 2235.
[43] Murray, C. B., Norris, D. J. and Bawendi, M. G., 1993, *J. Am. Chem. Soc.*, **115**, 8706.
[44] Kershaw, S. V., Burt, M., Harrison, M., Rogach, A., Weller, H. and Eychmüller, A., 1999, *Appl. Phys. Lett.*, **75**, 1694.
[45] Bruchez Jr., M., Moronne, M., Gin, P., Weiss, S. and Alivisatos, A. P., 1998, *Science*, **281**, 2013.
[46] Empedocles S. A. and Bawendi, M. G., 1997, *Science* **278**, 2114.
[47] Arakawa Y. and Sakaki, H., 1982, *Appl. Phys. Lett.*, **40**, 939.
[48] Bimberg, D., Grundmann, M. and Ledentsov, N. N., 1998, *Quantum Dot Heterostructures* (New York: Wiley).
[49] Maximov, M. V., Kochnev, I. V., Shernyakov, Y. M., Zaitsev, S. V., Gordeev, N. Yu., Tsatsul'nikov, A. F., Sakharov, A. V., Krestnikov, I. L., Kop'ev, P. S., Alfreov, Z. I., Ledentsov, N. N., Bimberg, D., Kosogov, A. O., Werner, P. and Gösele, U., 1997, *Jpn. J. Appl. Phys.*, **36**, 4221.
[50] Bouwmeester, D., Ekert, A. and Zeilinger, A., 2000, *The Physics of Quantum Information* (Berlin: Springer).
[51] Lounis, B. and Moerner, W. E., 2000, *Nature*, **407**, 491.
[52] Gérard J. M. and Gayral, B., 1999, *J. Lightwave Technology*, **17**, 2089.
[53] Santori, C., Pelton, M., Solomon, G., Dale, Y. and Yamamoto, Y., 2001, *Phys. Rev. Lett.*, **86**, 1502.
[54] Michler, P., Kiraz, A., Becher, C., Schoenfeld, W. V., Petroff, P. M., Zhang, L., Hu, E. and Imamoğlu, A., 2000, *Science*, **290**, 2282.
[55] Gérard, J. M., Sermage, B., Gayral, B., Legrand, B., Costard, E. and Thierry-Mieg, V., 1998, *Phys. Rev. Lett.*, **81**, 1110.
[56] Pettersson, H., Pryor, C., Landin, L., Pistol, M.-E., Carlsson, N., Seifert, W. and Samuelson, L., 2000, *Phys. Rev. B.*, **61**, 4795.
[57] Muto, S., 1995 *Jpn. J. Appl. Phys.*, **34**, L210.
[58] Lundstrom, T., Schoenfeld, W., Lee, H. and Petroff, P. M., 1999, *Science*, **286**, 2312.
[59] Haft, D., Warburton, R. J., Karrai, K., Huant, S., Medeiros-Ribeiro, G., Garcia, J. M., Schoenfeld, W. and Petroff, P. M., 2001, *Appl. Phys. Lett.*, **78**, 2946.
[60] Yusa G. and Sakaki, H., 1997, *Appl. Phys. Lett.*, **70**, 345.
[61] Finley, J. J., Skalitz, M., Arzberger, M., Zrenner, A., Böhm, G. and Abstreiter, G., 1998, *Appl. Phys. Lett.*, **73**, 2618.
[62] Shields, A. J., O'Sullivan, M. P., Farrer, I., Ritchie, D. A., Hogg, R. A., Leadbeater, M. L., Norman, C. E. and Pepper, M., 2000, *Appl. Phys. Lett.*, **76**, 3673.

Richard J. Warburton (RJW) studied for a DPhil at the Clarendon Laboratory, Oxford University (1987–1991), and was subsequently (1990–1993) a Junior Research Fellow at Christ Church, Oxford. At the end of 1993, RJW moved to the Faculty of Physics of the Ludwig-Maximilians-University (LMU), Munich, Germany, initially as a von Humboldt Fellow, and subsequently as a Marie-Curie Research Fellow. RJW became an Assistant Professor at the LMU in 1996, completing his *Habilitation* in 2000. Since 2000, he has been at the Department of Physics, Heriot-Watt University, Edinburgh.